# Refolding of autodisplayed anti-NEF scFv through oxidation with glutathione for immunosensors

Ji-Hong Bong, Hyun-Woo Song, Tae-Hun Kim, Min-Jung Kang, Joachim Jose, Jae-Chul Pyun

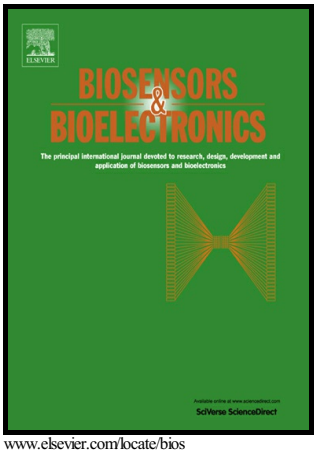


www.elsevier.com/locate/bios

PII: S0956-5663(17)30807-2
DOI: https://doi.org/10.1016/j.bios.2017.12.009
Reference: BIOS10154

To appear in: *Biosensors and Bioelectronic*

Received date: 30 July 2017
Revised date: 12 November 2017
Accepted date: 5 December 2017

Cite this article as: Ji-Hong Bong, Hyun-Woo Song, Tae-Hun Kim, Min-Jung Kang, Joachim Jose and Jae-Chul Pyun, Refolding of autodisplayed anti-NEF scFv through oxidation with glutathione for immunosensors, *Biosensors and Bioelectronic,* https://doi.org/10.1016/j.bios.2017.12.009

# Refolding of autodisplayed anti-NEF scFv through oxidation with glutathione for immunosensors

Ji-Hong Bong[1], Hyun-Woo Song[1], Tae-Hun Kim[1], Min-Jung Kang[2], Joachim Jose[3], Jae-Chul Pyun[1,*]

[1]Department of Materials Science and Engineering, Yonsei University

50 Yonsei-Ro, Seodaemun-Gu, Seoul, 120-742, Korea

Tel) 82 2 2293 5509 / Fax) 82 2 312 5375 / Email) jcpyun@yonsei.ac.kr

[2] Korea Institute of Science and Technology (KIST), Seoul, Korea

[3] Muenster University, Muenster, Germany

* To whom correspondence should be addressed

**Abstract**

In this study, a single-domain antibody against negative regulatory factor (anti-NEF scFv) was autodisplayed on the outer membrane of *Escherichia coli* and used to detect NEF in an immunoassay based on fluorescence-activated cell sorting, enzyme-linked immunosorbent assay, and surface plasmon resonance biosensors. Next, the autodisplayed single-domain antibody was oxidized to form disulfide bonds by using glutathione, and the change in NEF-binding activity of anti-NEF scFv was analyzed by fluorescence-activated cell sorting-based immunoassay, chromogenic immunoassay, and surface plasmon resonance biosensor. For each type of immunoassays the anti-NEF scFv on the isolated outer membrane showed more NEF binding activity after the disulfide bond formation by glutathione. To determine the role of cysteines in anti-NEF scFv, three mutants were prepared, and the NEF binding activity of mutants was compared with that of wild-type anti-NEF scFv in a competitive immunoassay based on FACS. In these mutant studies, the refolding process of autodisplayed anti-NEF scFv by following oxidation via GSH/GSSG revealed that disulfide bonds formed and increased NEF binding activity.

**Keywords:** negative regulatory factor (NEF), autodisplay, single-chain variable fragment (scFv), glutathione, immunoassay

## 1. Introduction

Negative regulatory factor (NEF) is a capsid protein of human immunodeficiency virus and is used as a biomarker to diagnose acquired immunodeficiency syndrome. The capture antibody against NEF was made using a heptapeptide of NEF as an epitope of a monoclonal antibody (Spohn et al. 1992). The monoclonal antibody against NEF was genetically analyzed by reverse transcription of total RNA of the hybridoma cell to obtain the cDNA of antibody fragments (Kay et al. 1996). As shown in Fig. 1(a), a single-domain antibody (scFv) against NEF was constructed by connecting two Fab regions of heavy and light chains (Juillerat et al. 2016; Sepulveda and Shoemaker 2008; Ward et al. 1989). In this study, the scFv against NEF was expressed on the outer membrane of *Escherichia coli* using autodisplay technology.

Autodisplay technology is a method used to express a target protein (Jose et al. 2009; Park et al. 2010; Yoo et al. 2015a). When the target protein gene is inserted as a passenger in an autodisplay vector composed of the autotransporter protein AIDA-1, the target protein is expressed on the outer membrane of *E. coli* as a fusion protein of AIDA-1, which is a transmembrane beta-barrel that transports the target protein from the periplasm to the outer membrane of *E. coli* (Fig. 1(b)). The autodisplay technology can be used to express a target protein on the outer membrane of *E. coli* with a surface density as high as $10^5$ proteins/*E. coli*. Additionally, multimeric proteins can be expressed as a single-domain protein via a peptide linker, such as the single-domain antibody composed of heavy and light chains of the antibody Fab region. Many types of proteins have been autodisplayed, including Z-domain (Kim et al. 2016a; Kim et al. 2016b; Yoo et al. 2013; Yoo et al. 2011), streptavidin (Park et al. 2011b), Ro/SSA (Petermann et al. 2010;

Yoo et al. 2014), La/SSB (Yoo et al. 2017), casein (Yoo et al. 2015b), lipase, and foldase (Chang et al. 2017), among others. Prepared autodisplayed proteins can be used in immunoassays by using whole *E. coli* (Jose et al. 2010; Lee et al. 2012; Park et al. 2014; Park et al. 2013; Park et al. 2011a; Pyun et al. 2017) and by separating the outer membrane with autodisplayed proteins and layering on sensor surfaces (Jose et al. 2009; Park et al. 2010). When a target protein contains disulfide bonds such as antibodies (IgGs), the autodisplay typically has difficulty transporting expressed proteins to the outer membrane of *E. coli* through the beta-barrel of AIDA-1. Because of the restricted autotransport of expressed proteins with disulfide bonds, autodisplay of a target protein has been carried out under reducing conditions with beta-mercaptoethanol. As shown in Fig. 1(c), anti-NEF scFv also contains five cysteine residues that can form disulfide bonds within scFv, which typically form following expression involving oxidation reactions, such as glutathione (GSH) and its oxidized form (GSSG) (Cowgill et al. 2007; Wingfield et al. 2001). This work presented that the oxidation of autodisplayed single-domain antibody could improve the binding activity by formation of disulfide bonds. In this study, a single-domain antibody against NEF was autodisplayed on the outer membrane of *E. coli* and was used to detect NEF by using an immunoassay based on fluorescence-activated cell sorting (FACS) (Park et al. 2014; Park et al. 2013; Pyun et al. 2017), enzyme-linked immunosorbent assay (ELISA) (Jose et al. 2009; Park et al. 2010), and surface plasmon resonance (SPR) biosensors (Jose et al. 2010; Lee et al. 2012; Park et al. 2011a). For mutant studies, candidate cysteine residues involved in disulfide bond formation were analyzed.

## 2. Materials and methods

### 2.1 Materials

High-salt Luria-Bertani (LB) medium was purchased from Duchefa (Haarlem, Netherlands). Heptapeptide of NEF (GAASRDL) and modified peptides were synthesized with purities of 95% by Peptron Co. (Daejeon, Korea). Oligonucleotides were synthesized by Macrogen, Inc. (Seoul, Korea). Oxidized and reduced forms of glutathione and all other chemical reagents were from Sigma-Aldrich (St. Louis, MO, USA). 3,3′,5,5′-Tetramethylbenzidine was purchased from Pierce Co. (Rockford, IL, USA). High-fidelity Phusion polymerase and all other PCR reagents were purchased from Thermo Fisher Scientific, Inc. (Waltham, MA, USA).

### 2.2 Autodisplay of scFv against NEF

To autodisplay anti-NEF scFv, competent cells of intact *E. coli* BL21 (DE3) were transformed with the autodisplay vector pFB006. This modified pET-11d-based vector (pET-SH3SDH08) vector contains the AIDA-1 autotransporter and signal peptide of a cholera toxin B subunit; the linker region between the β-barrel and target protein sequence was differently modified to control the levels of autodisplayed proteins (Jose et al. 2009; Park et al. 2010; Yoo et al. 2015a; Yoo et al. 2013; Yoo et al. 2011). The AIDA-I autotransporter is expressed under control of the T7/lac promoter. Next, intact *E. coli* and lipopolysaccharide-free *E. coli* were grown in high-salt LB medium (20 mL) containing 50 mg $L^{-1}$ carbenicillin at 37°C (overnight culture). For the main culture, intact *E. coli* cells

were incubated in high-salt LB medium (100 mL) containing carbenicillin (50 mg $L^{-1}$), ethylenediaminetetraacetate (EDTA, 10 μM), and beta-mercaptoethanol (10 mM) at 37°C with shaking until the OD600 reached 0.6 (Jose et al. 2009; Kim et al. 2016a; Kim et al. 2016b; Park et al. 2010; Ward et al. 1989; Yoo et al. 2015a; Yoo et al. 2013; Yoo et al. 2011). To express anti-NEF scFv, intact *E. coli* cells were induced with 1 mM isopropyl-D-1-thiogalactopyranoside (IPTG) and grown at 37°C for 1 h with shaking. In this study, the densitometry of SDS-PAGE was used to quantify the number of expressed proteins on the outer membrane of *E. coli*. The band densities of Omp C and scFv proteins were analyzed by using a commercial documentation system (Chemi-Doc XRS™, Bio-Rad, Hercules, CA, USA) and the expression level was calculated using a commercial program (Quantity-One™, Bio-Rad). The harvested *E. coli* cells were resuspended in 0.2 M Tris-HCl buffer (pH 8.0). To isolate the outer membrane, 200 μg $mL^{-1}$ lysozyme, 20 mM sucrose, and 0.2 mM EDTA were added followed by incubation for 10 min at room temperature. Next, 1 mM phenylmethylsulfonyl fluoride, aprotinin (20 μg $mL^{-1}$), and extraction buffer (2 % Triton X-100, 50 mM Tris-HCl, and 10 mM $MgCl_2$) were added and incubated for 25 min at 4°C. The cell lysates were centrifuged at 17,000 ×*g* for 5 min at 4°C. After the supernatants were centrifuged at 48,640 ×*g* for 10 min at 4°C, the pellets were washed twice with PBS and resuspended in 100 μL PBS.



**2.3 Immunoassays with scFv against NEF**

The *E. coli* cells with autodisplayed anti-NEF scFv were reacted with various concentrations of modified NEF peptides and incubated for 1 h at room temperature in

PBS or spiked into 100-fold diluted serum. After NEF peptide binding, the cells were washed three times with 1 mL PBS and evaluated by flow cytometry.

For the ELISA tests, *E. coli* was immobilized on microplates by incubation in microplate wells with modified surfaces (Jose et al. 2010; Lee et al. 2012; Park et al. 2014; Park et al. 2013; Park et al. 2011a; Pyun et al. 2017). Polystyrene microplates were coated with parylene-H film using a parylene coater from FemtoScience Co. (Seoul, Korea). The parylene precursors of parylene-H were supplied by FemtoScience Co. The deposition of parylene-H film was controlled to achieve a final thickness of 20 nm by adjusting the initial amount of parylene-H precursors to 50 mg (Jeon et al. 2011; Jung et al. 2014; Ko et al. 2011; Yoo et al. 2011). To immobilize poly-L-lysine on the microplate, poly-L-lysine solution (Sigma-Aldrich) was applied for 2 h. After washing, *E. coli* were incubated in each well for 2 h. NEF peptides were mixed with various concentrations of biotinylated NEF peptides and incubated for 1 h at room temperature. Horseradish peroxidase (HRP)-conjugated NEF peptides were added to each sample and allowed to react for 1 h at room temperature. Finally, 3,3′,5,5′-tetramethylbenzidine solution (Pierce) was used in the chromogenic reaction. After quenching with 2 M sulfuric acid as a stop solution, the OD450 value was measured on a microplate reader (Molecular Devices, Sunnyvale, CA, USA) (Jose et al. 2009; Park et al. 2010).

An SPR biosensor with a lab-made SPR chip was used to determine autodisplayed anti-NEF scFv activity in the OM layer. The SPR chip was fabricated by sputtering an adhesive layer of titanium (2 nm) followed by a layer of gold (48 nm) on BK-7 glass (10 × 10 $mm^2$). An SPR biosensor from KMac Co. (Yousung, Korea) was used as previously described

(Jose et al. 2010; Lee et al. 2012; Park et al. 2011a). Sample solution and washing buffer were injected into the sensor chip using an injection valve and peristaltic tubing pump. The flow rate was controlled (1 mL/min), and solution flow was stopped by regulating the peristaltic tubing pump during incubation. To detect the activity of an OM protein by measuring the SPR signal, OM fractions with autodisplayed anti-NEF scFv were injected into the SPR chip to prepare the OM layer. For the OM layer preparation OM fraction at the concentration of 0.1 mg/ml was treated for 2 h on the gold surface of SPR sensor. And the, the SPR chip was washed three times with PBS. Various concentrations of magnetic beads combined with NEF peptide were injected for 1 min and incubated for 20 min. The NEF peptide was immobilized on the magnetic bead with streptavidin from Invitrogen (Carlsbad, CA, USA). For the immobilization reaction, biotin labeled NEF solution at the concentration of 1 mg/ml (100 μl in PBS) was mixed with magnetic beads (1 mg in 100 μl) for 2 h at room temperature. After five times of washing, the magnetic bead with NEF peptide was used for SPR measurement. Finally, the SPR signal was calculated by comparison of signals before and after protein injection (Lee et al. 2017).



**2.4 Preparation of mutants of scFv against NEF**

The autodisplay vector pFB006 was modified by PCR with various primers to substitute cysteine candidates with alanine residues. For substitution of the first cysteine residue in the light chain region, the forward primer JB001_F (5′-AGTCTCCATCTCTGCTAGATCTAG-TCAGAGCA-3′) and reverse primer JB001_R (5′-TGCTCTGACTAGATCTAGCAGAG-ATGGAGACT-3′) were used for PCR. For substitution of the fifth cysteine residue, forward

primer JB005_F (5′-GCGGTCTATTACGCTGCAAGAGAACC-3′) and reverse primer JB005_R (5′-GGTTCTCTTGCAGCGTAATAGACCGC-3′) were used. Finally, to insert a Tev protease cleavage site, primer JB_TEV_ins_R (5′-ACCAGACG-GTCCGTGGATTGGAAGTACAGGTTCTCAAGTGAATTATCT-3′) was used. PCR was performed according to protocol for high-fidelity DNA polymerase: (1) 98°C for 1 min; (2) 98°C for 30 s; (3) 68°C for 1 min; (4) 72°C for 5 min; (5) repeat for 30 cycles from step (2) to step (5); (6) 72°C for 10 min; (7) hold at 4°C. The remaining template was digested by DpnI enzyme at 37°C for 20 min and subsequently inactivated at 80°C for 20 min. The PCR product was dialyzed in a nitrocellulose membrane for 45 min. Dialyzed PCR product was transformed into freshly prepared electrocompetent cells of *E. coli* BL21 (DE3). These cells were grown overnight on an agar plate containing carbenicillin and the genetic sequence of the colonies was analyzed (Li and Fan 2017; Li et al. 2016).



**2.5 Calculation of affinity parameters**

Affinity parameters were calculated using the Cheng and Prussoff correlation (1973) for the affinity binding of ligands to receptors in competitive immunoassays (Hulme and Trevethick 2010):

$$K_d = \frac{IC_{50}}{1 + L_T/K_{d.L}}$$

where $K_d$ is the dissociation constant for NEF peptide; $K_{d.L}$ represents the dissociation constant for labeled NEF peptide; $L_T$ represents the total concentration of labeled NEF peptide; and $IC_{50}$ represents the concentration of NEF peptide that yields 50% binding in

the presence of a given concentration of NEF peptide. Fitting of the assay results was carried out to determine the response maximum ($R_{max}$), response minimum ($R_{min}$), and $IC_{50}$ by using the four-parameter logistic model (Findlay and Dillard 2007).

## 3. Results and discussion

### 3.1 Autodisplay of anti-NEF scFv

The single-domain antibody (scFv) was prepared by connecting the Fab region of the light and heavy chains of monoclonal anti-NEF antibody with a peptide linker (15 residues). As shown in Fig. 1(c), two cysteine residues were present in both the heavy and light chains and one cysteine residue in the peptide linker contained a cleavage site (E/NLYFQS) for Tev protease. These five cysteine residues can form disulfide bonds after autodisplay through an oxidation reaction, such as by using GSH and GSSG. Both the heavy and light chains contain three complementarity determining regions that can directly interact with NEF.

Autodisplay of anti-NEF scFv was analyzed by SDS-PAGE. As shown in Fig. 2(a), anti-NEF scFv was expressed following IPTG induction (lane 3). When the linker site between autodisplayed anti-NEF scFv and the beta-barrel of AIDA-1 by proteinase K, the protein band of anti-NEF scFv was significantly fainter (lane 2). When IPTG induction was not carried out, no protein band was observed for the autodisplay of anti-NEF scFv (lane 1). These results demonstrate that anti-NEF scFv was autodisplayed on the outer membrane

of *E. coli* following IPTG induction, and the surface density of autodisplayed anti-NEF scFv was estimated to be $10^5$ scFv/*E. coli* based on densitometric analysis of protein bands with the reference protein band of Omp C (38 kDa, $10^5$ protein/*E. coli*) (JC et al. 2016). The autodisplay of anti-NEF scFv contains a cleavage site (E/NLYFQS) for Tev protease at the peptide linker between scFv and beta-barrel of AIDA-1. As shown in Fig. 2(b), two protein bands of scFv (32.72 kDa) and beta-barrel of AIDA-1 (44.7 kDa) were observed after treatment with Tev protease. The protease activity of Tev was also confirmed in a model fusion protein composed of maltose-binding protein and eGFP. Because the two proteins were connected by a peptide linker containing a cleavage site, protein bands for maltose-binding protein and eGFP were observed after the reaction with Tev. These results also showed that anti-NEF scFv was autodisplayed on the outer membrane of *E. coli* by IPTG induction.

### 3.2 Influence of disulfide formation on anti-NEF scFv activity

As described above, autodisplayed proteins can be effectively used in immunoassays because the autodisplay technology can express target proteins with a high surface density and the negatively charged outer membrane of *E. coli* reduces the non-specific binding of proteins. The *E. coli* with autodisplayed anti-NEF scFv can be used for an immunoassay of NEF by using a competitive assay format. In this study, the fluorescence labeled NEF with TAMRA ($\lambda_{EX}$=546, $\lambda_{EX}$=579) at a fixed concentration of 414.8 nM was mixed with NEF (analyte) samples of known concentration, and the sample solution was reacted with *E. coli* with autodisplayed anti-NEF scFv. When anti-NEF antibody was

oxidized by treatment with GSH and GSSG, the disulfide bonds in scFv were considered to have formed. The refolded (oxidized) amount of bound TAMRA-labeled NEF was decreased with increasing concentrations of NEF and the fluorescence signal in FACS analysis was decreased. As shown in Fig. 3(b), this concentration-dependent change in NEF in FACS analysis was observed for samples in PBS as well as in serum. For samples in serum, fluorescence signals ranged from 400 to baseline at NEF concentrations of 50 nM–500 μM. The same fluorescence signal range was observed for the sample in serum at NEF concentrations of 0.5 μM–5 mM. These results demonstrate that the fluorescence signal from the sample in serum was reduced by approximately 10-fold compared with that from the sample in PBS.

When anti-NEF antibody was applied in the same competitive immunoassay based on FACS before treatment with GSH and GSSG, the change in the fluorescence signal indicating the amount of bound TAMRA-labeled NEF was not significantly decreased with increasing concentrations of NEF compared to refolded (oxidized) scFv. As shown in Fig. 3(c), the results of immunoassays based on autodisplayed anti-NEF scFv before and after refolding (oxidation) were compared for samples in PBS and in serum. When samples in PBS was compared, the immunoassays based on autodisplayed anti-NEF scFv after refolding (oxidation) showed three-fold higher sensitivity than unfolded (unoxidized) anti-NEF scFv. The detection range for both of immunoassays was estimated to be in a dynamic range from less than 10 nM to 1 mM, and both immunoassays had a limit of detection of less than 20 nM and dissociation constant of 475 nM. For samples in serum, the sensitivity of both of immunoassays was approximately 30% lower than that for

samples in PBS. These results demonstrate that the refolding process improved the NEF binding activity of the autodisplayed anti-NEF scFv via disulfide bond formation.

The influence of pH on the binding activity of anti-NEF antibody was estimated before and after treatment with GSH and GSSG by using TAMRA-labeled NEF at the concentration of 400 nM as an analyte. As shown in Fig. 3(d), the optimal pH for the binding activity was estimated for both of anti-NEF antibodies before and after treatment with GSH and GSSG in the pH range of 3 – 11. The anti-NEF antibody before and after the oxidation reaction showed the optimal binding activity in the pH range of 6 – 9 and 5- 11, respectively. Such results was represented that disulfide bond was known to be easily formed and stable at basic pH (Trivedi et al. 2009). And, the binding activity was observed to be increased after the oxidation reaction. Therefore, the scFv could be more effectively applied for the binding of analyte at physiological pH condition after the oxidation reaction with GSH and GSSG.

The autodisplayed proteins can be applied in ELISAs by immobilizing *E. coli* cells on the surface of a microplate. To effectively immobilize *E. coli* which has a negatively charged outer membrane, the surface of the microplate was modified to have a highly positive charge by using parylene and poly-lysine coating. As shown in Fig. 4(a), a competitive immunoassay was carried out by mixing HRP-labeled NEF and a sample containing NEF (analyte). The amount of NEF (analyte) was visualized as a chromogenic reaction between HRP and 3,3′,5,5′-tetramethylbenzidine. After quenching the enzyme reaction, the optical density was measured at a wavelength of 450 nm. As shown in Fig. 4(b), the competitive assay was carried out at an NEF (analyte) concentration range of 10 nM–1 mM by using

unfolded and refolded anti-NEF scFv. The sensitivity of the immunoassay based on refolded anti-NEF scFv was three-fold higher than that of the unfolded anti-NEF scFv. The dynamic range of NEF was 100 nM–100 μM for both immunoassays. These results demonstrate that refolded anti-NEF scFv is more suitable for chromogenic immunoassays because of the improved NEF binding activity compared to the unfolded sample.

The autodisplayed proteins on the outer membrane of *E. coli* can also be applied by isolating the outer membrane and then layering the membrane on the hydrophobic surface of sensors. In this study, the outer membrane of *E. coli* with autodisplayed anti-NEF scFv was isolated and layered on an SPR biosensor to compare the refolding (oxidation) process. As shown in Fig. 5(a), NEF samples at known concentrations of NEF in the range of 0.33–26.7 nM were injected and then, signals were acquired after three washes. As a negative control, the outer membrane of *E. coli* without autodisplayed proteins was coated on an SPR biosensor. As shown in Fig. 5(a), the SPR sensorgrams from the SPR biosensor with refolded anti-NEF scFv showed a higher sensor response compared to those with unfolded anti-NEF scFv and intact one. As shown in Fig. 5(b), a difference in sensitivity between unfolded and refolded anti-NEF scFv was observed at NEF concentrations as low as 10 nM. These results show that refolded anti-NEF scFv on the isolated outer membrane may have greater NEF binding activity than unfolded anti-NEF scFv.



### 3.3 Studies of anti-NEF scFv mutants

Autodisplay technology transports a target protein from the periplasm to the outer

membrane through the beta-barrel of AIDA-1. Because the expressed protein should penetrate the beta-barrel, autodisplay of a target protein is carried out under reducing conditions in the presence of beta-mercaptoethanol. Usually, each $V_H$ and $V_L$ chain has one intra-domain disulfide bond, and the reduction of the disulfide bond were known to result in a large conformational change (Litman et al. 1970). Additionally, irreversible inactivation of binding activity as well as aggregation were reported to be occurred (Glockshuber et al. 1992). The exchange of Cys23 to Val also shown to reduce the stability of antibodies (Frisch et al. 1996). These reports represented the relation between the disulfide bonds and the binding activity of antibodies. As shown in Fig. 6(a), anti-NEF scFv contains two cysteine residues in the light chain and heavy chain regions, which can form disulfide bonds. Typically, antibodies in IgG forms contain disulfide bonds between these two residues. After autotransport of scFv to the outer membrane, two disulfide bonds between Cys-48 and Cys-118 in the light chain region as well as between Cys-178 and Cys-252 in the heavy chain regions were expected to be formed during refolding via oxidation of scFv by using GSH/GSSG.

Computer simulation of the amino acid sequence of anti-NEF scFv was conducted to construct a thermodynamically stable structure by using SWISS-MODEL Workspace (https://swissmodel.expasy.org/interactive) (Biasini et al. 2014). As shown in Fig. 6(b), the stable structure of anti-NEF scFv was analyzed to ensure that Cys-48 and Cys-118 in the light chain and Cys-178 and Cys-252 in the heavy chain were very closely positioned. The stability constants (QMEAN value) for the light chain and heavy chain regions were calculated to be 0.44 and 0.17, respectively, showing high consistency with the model

crystal structures (Benkert et al. 2010). These results indicate that the formation of disulfide bonds after GSH/GSSG in the light chain and heavy chain regions of anti-NEF scFv. To determine the role of cysteines in anti-NEF scFv, three mutants were prepared as shown in Fig. 6(c) and Supplement: mutant 1 with Cys-48 converted to Ala-48, mutant 2 with Cys-252 converted to Ala-252, mutant 3 with Cys-48 converted to Ala-48 and Cys-252 to Ala-252. Next, the NEF binding activities of the mutants were compared with that of wild-type anti-NEF scFv in a competitive immunoassay using FACS as shown in Fig. 6(d). The competitive assay was carried out at an NEF concentration range of 10 nM–100 μM and at a fixed concentration of fluorescence-labeled NEF of 414.8 nM. As shown in Fig. 6(e), wild-type anti-NEF scFv showed a dynamic range of 50 nM–50 μM and a detection limit of 18 nM. However, mutant 1 scFv showed a dynamic range of 5–50 μM and a detection limit of 4.88 μM. Mutants 2 and 3 showed nearly no response at the NEF concentration range in the immunoassay. These results demonstrate that the mutation of cysteine residues of wild-type scFv significantly reduced sensitivity. Mutation of cysteine residues in the heavy chain region of scFv reduced sensitivity to a significantly greater extent than mutation in the light chain region. Therefore, the refolding of autodisplayed anti-NEF scFv via oxidation by GSH/GSSG may promote disulfide bond formation and increase NEF binding activity.



**Conclusions**

A single-domain antibody (scFv) was prepared by connecting the Fab region of the light and heavy chains of a monoclonal anti-NEF antibody with a peptide linker (15 residues)

containing a cleavage site (E/NLYFQS) for Tev protease. Anti-NEF scFv was autodisplayed on the outer membrane of *E. coli* by IPTG induction, which can be used for immunoassays of NEF with a competitive assay format. When anti-NEF antibody was oxidized by treatment with GSH and GSSG, disulfide bonds in scFv were formed. For refolded (oxidized) anti-NEF scFv, the amount of bound TAMRA-labeled NEF was decreased with increasing concentrations of NEF and the fluorescence signal in FACS analysis was decreased. The autodisplayed proteins can be applied in ELISA by immobilizing *E. coli* cells on the microplate surface, and refolded anti-NEF scFv may be effective for use in chromogenic immunoassays based on the improved NEF binding activity compared to unfolded anti-NEF scFv. Autodisplayed proteins on the outer membrane of *E. coli* may also be applied by isolating the outer membrane and then layering on the hydrophobic surface of the sensors. In this study, the outer membrane of *E. coli* containing autodisplayed anti-NEF scFv was isolated and layered on an SPR biosensor. For SPR biosensor analysis, refolded anti-NEF scFv on the isolated outer membrane showed more NEF binding activity than unfolded anti-NEF scFv. To determine the role of cysteines in anti-NEF scFv, three mutants were prepared, and the NEF binding activity of mutants was compared with that of wild-type anti-NEF scFv in a competitive immunoassay based on FACS. In these mutant studies, the refolding process of autodisplayed anti-NEF scFv by following oxidation via GSH/GSSG revealed that disulfide bonds formed and increased NEF binding activity.



**Acknowledgements**

Funding: This work was supported by the Nano-Convergence Foundation [grant number: R201602210] funded by the Ministry of Science, ICT and Future Planning (MSIP, Korea) and Ministry of Trade, Industry and Energy (MOTIE, Korea), Industry Technology Development Program [grant number: 10063335] funded by the Ministry of Trade, Industry and Energy (MOTIE, Korea), and National Research Foundation of Korea [grant numbers: NRF-2017R1A2B4004077, NRF-2017R1A2B2004398].

**Figure legends**

Fig. 1. Autodisplay of anti-NEF scFv. (a) Schematic view of autodisplayed anti-NEF scFv. (b) Amino acid sequence of anti-NEF scFv with five cysteine residues.

Fig. 2. SDS-PAGE analysis of autodisplayed anti-NEF scFv. (a) Autodisplayed anti-NEF scFv before and after treatment with IPTG and proteinase K. (b) Cleavage of autodisplayed anti-NEF scFv with Tev proteinase. (c) Autodisplayed anti-NEF scFv before and after refolding with GSH/GSSG.

Fig. 3. Competitive immunoassay based on FACS with autodisplayed anti-NEF scFv before and after refolding. (a) Schematic view of competitive assay with anti-NEF scFv. (b) Results of competitive immunoassay with autodisplayed anti-NEF scFv before and after refolding. (c) Comparison of results of competitive immunoassay with autodisplayed anti-NEF scFv before and after refolding. (d) Influence of pH on the binding activity of anti-

NEF antibody before and after oxidation process of GSH and GSSG.

Fig. 4. Competitive ELISA with autodisplayed anti-NEF scFv before and after refolding. (a) Schematic view of competitive assay with anti-NEF scFv. (b) Comparison of results for competitive immunoassay with the autodisplayed anti-NEF scFv before and after refolding.

Fig. 5. Competitive immunoassay based on SPR biosensor with autodisplayed anti-NEF scFv before and after refolding. (a) Sensorgram of competitive assay with anti-NEF scFv. (b) Comparison of results for competitive immunoassay with autodisplayed anti-NEF scFv before and after refolding.

Fig. 6. Mutant study to determine the role of cysteine residues in autodisplayed anti-NEF scFv. (a) Schematic view of autodisplayed anti-NEF scFv with five positions of cysteine residues, and disulfide bonds after refolding with GSH/GSSG. (b) Simulation of the position of cysteine residues from the analysis of amino acid sequence of autodisplayed anti-NEF scFv. (c) Amino acid sequences of wild-type and three mutants of anti-NEF scFv. (d) Schematic view of competitive assay with wild-type and mutant anti-NEF scFvs. (e) Comparison of results for competitive immunoassay with wild-type and mutant anti-NEF scFvs.

Supplement. Amino acid sequences of three mutants of anti-NEF scFvs.

## References

Benkert, P., Biasini, M., Schwede, T., 2010. Bioinformatics 27(3), 343-350.

Biasini, M., Bienert, S., Waterhouse, A., Arnold, K., Studer, G., Schmidt, T., Kiefer, F., Cassarino, T.G., Bertoni, M., Bordoli, L., 2014. Nucleic Acids Res, gku340.

Chang, S.-Y., Bong, J.-H., Yoo, G., Lee, M., Kang, M.-J., Jose, J., Pyun, J.-C., 2017. Enzyme Microb. Technol. 96, 85-95.

Cowgill, C., Ozturk, A.G., StJohn, R., 2007. BIOTECHNOLOGY AND BIOPROCESSING SERIES 31, 123.

Findlay, J.W., Dillard, R.F., 2007. The AAPS journal 9(2), E260-E267.

Frisch, C., Kolmar, H., Schmidt, A., Kleemann, G., Reinhardt, A., Pohl, E., Usón, I., Schneider, T.R., Fritz, H.-J., 1996. Fold Des. 1(6), 431-440.

Glockshuber, R., Schmidt, T., Plueckthun, A., 1992. Biochemistry 31(5), 1270-1279.

Hulme, E.C., Trevethick, M.A., 2010. Br J Pharmacol 161(6), 1219-1237.

JC, I., Olayinka, B., Ehnimidu, J., Onaolapo, J., 2016.

Jeon, B.-J., Kim, M.-H., Pyun, J.-C., 2011. Sensors Actuators B: Chem. 154(2), 89-95.

Jose, J., Chung, J.-W., Jeon, B.-J., Maas, R.M., Nam, C.-H., Pyun, J.-C., 2009. Biosensors Bioelectron. 24(5), 1324-1329.

Jose, J., Park, M., Pyun, J.C., 2010. Biosensors Bioelectron. 25(5), 1225-1228.

Juillerat, A., Marechal, A., Filhol, J.-M., Valton, J., Duclert, A., Poirot, L., Duchateau, P., 2016. Sci. Rep. 6, 18950.

Jung, H.-W., Chang, Y.W., Lee, G.-y., Cho, S., Kang, M.-J., Pyun, J.-C., 2014. Anal. Chim. Acta 844, 27-34.

Kay, B.K., Winter, J., McCafferty, J., 1996. Phage display of peptides and proteins: a laboratory manual. Academic Press.

Kim, D.H., Bong, J.H., Yoo, G., Chang, S.Y., Chang, Y.W., Kang, M.J., Jose, J., Pyun, J.C., 2016a. Enzyme Microb. Technol. 92, 1-8.

Kim, D.H., Bong, J.H., Yoo, G., Chang, S.Y., Park, M., Chang, Y.W., Kang, M.J., Jose, J., Pyun, J.C., 2016b. Appl. Surf. Sci. 362, 146-153.

Ko, H., Lee, E.-H., Lee, G.-Y., Kim, J., Jeon, B.-J., Kim, M.-H., Pyun, J.-C., 2011. Biosensors Bioelectron. 30(1), 56-60.

Lee, E.-H., Yoo, G., Jose, J., Kang, M.-J., Song, S.-M., Pyun, J.-C., 2012. BioChip Journal 6(3), 221-228.

Lee, K., Kim, Y.-H., Jung, H., Lee, H.H., 2017. BioChip Journal 11(2), 131-138.

Li, Y.-J., Fan, J.-Y., 2017. BioChip Journal 11(1), 8-13.

Li, Y., Xiong, T., Wu, H., Yang, Y., 2016. BioChip Journal 10(1), 42-47.

Litman, G., Good, R., Frommel, D., Rosenberg, A., 1970. Proc. Natl. Acad. Sci. 67(3), 1085-1092.

Park, M., Bong, J.H., Chang, Y.W., Yoo, G., Jose, J., Kang, M.J., Pyun, J.C., 2014. Analytical Methods 6(6), 1700-1708.

Park, M., Bong, J.H., Yoo, G., Jose, J., Kang, M.J., Pyun, J.C., 2013. Enzyme Microb. Technol. 53(3), 181-188.

Park, M., Jose, J., Pyun, J.-C., 2011a. Sensors Actuators B: Chem. 154(2), 82-88.

Park, M., Jose, J., Pyun, J.C., 2010. Enzyme Microb. Technol. 46(3-4), 309-314.

Park, M., Jose, J., Thömmes, S., Kim, J.I., Kang, M.J., Pyun, J.C., 2011b. Enzyme Microb. Technol. 48(4-5), 307-311.

Petermann, K., Vordenbäumen, S., Pyun, J.-C., Braukmann, A., Bleck, E., Schneider, M., Jose, J., 2010. Anal Biochem 407(1), 72-78.

Pyun, J.-C., Jose, J., Park, M., 2017. Analyst 142(10), 1720-1728.

Sepulveda, J., Shoemaker, C.B., 2008. J. Immunol. Methods 332(1), 92-102.

Spohn, R., Gombert, F., Jung, G., 1992. Res Virol 143, 70-81.

Trivedi, M.V., Laurence, J.S., Siahaan, T.J., 2009. Curr. Protein Peptide Sci. 10(6), 614-625.

Ward, E.S., Güssow, D., Griffiths, A.D., Jones, P.T., Winter, G., 1989. Nature 341(6242), 544-546.

Wingfield, P.T., Palmer, I., Liang, S.M., 2001. Current protocols in protein science, 6.5. 1-6.5. 30.

Yoo, G., Bong, J.-H., Kim, S., Jose, J., Pyun, J.-C., 2014. Biosensors Bioelectron. 57, 213-218.

Yoo, G., Bong, J.H., Park, M., Jose, J., Kang, M.J., Pyun, J.C., 2015a. Biochimica Et Biophysica Acta-Biomembranes 1848(7), 1509-1513.

Yoo, G., Bong, J.H., Park, M., Kang, M.J., Jose, J., Pyun, J.C., 2013. Enzyme Microb. Technol. 53(2), 118-122.

Yoo, G., Dilkaute, C., Bong, J.-H., Song, H.-W., Lee, M., Kang, M.-J., Jose, J., Pyun, J.-C., 2017. Enzyme Microb. Technol. 100, 1-10.

Yoo, G., Park, M., Lee, E.-H., Jose, J., Pyun, J.-C., 2011. Anal. Chim. Acta 707(1), 142-147.

Yoo, G., Saenger, T., Bong, J., Park, M., Jose, J., Kang, M., Pyun, J., 2015b. Biochim Biophys Acta Biomembr 1848, 3126-3133.

**Highlights**

• Anti-NEF scFv was autodisplayed on the outer membrane (OM) of *Escherichia coli*.

• Autodisplayed anti-NEF scFv was oxidized to form disulfide bonds by using glutathione.

• The activity of scFv was analyzed by FACS-based immunoassay and SPR biosensor.

• Mutants were made to confirm the formation of disulfides after the reaction of glutation.



Fig. 1

(a)

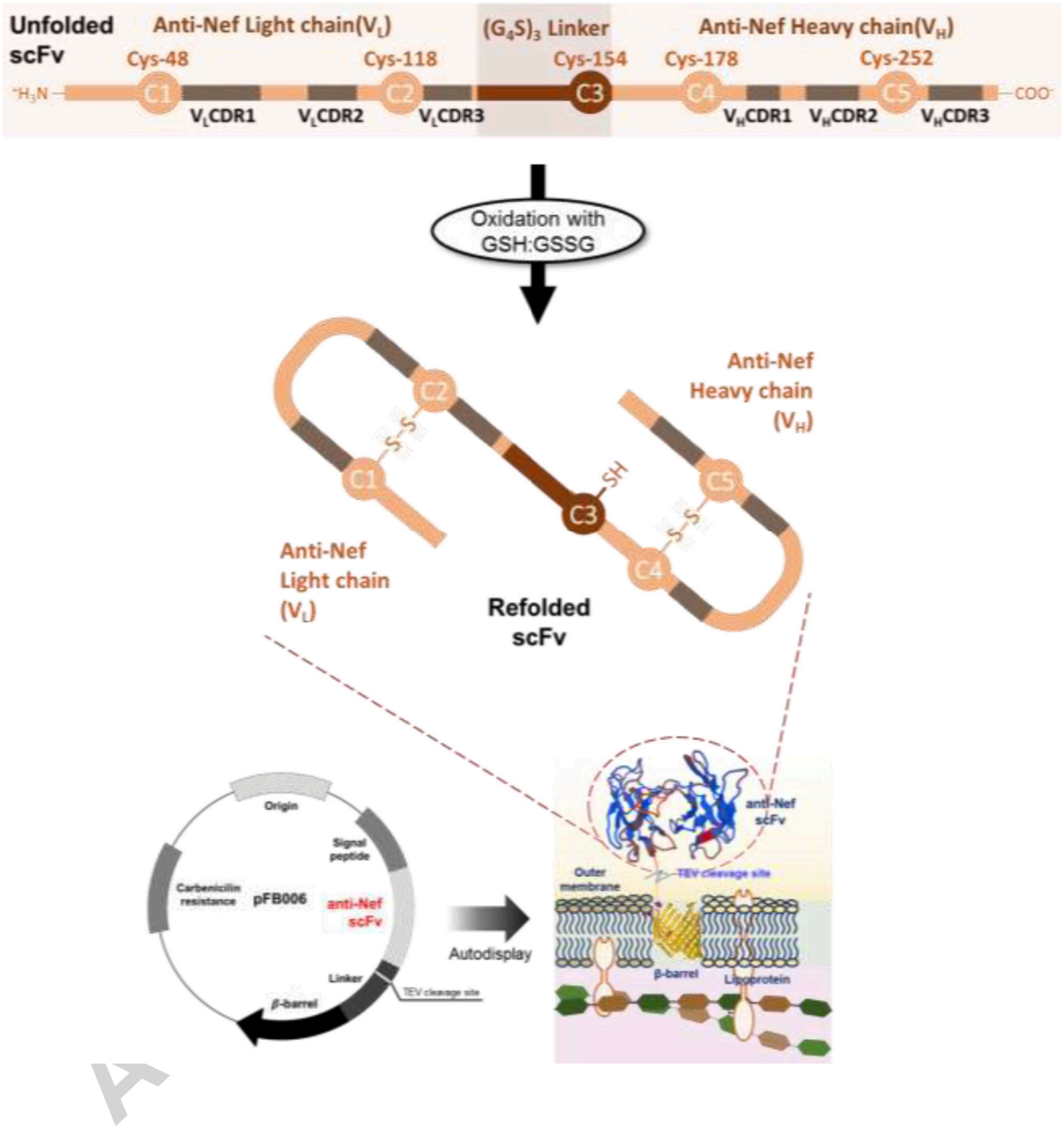
Unfolded scFv
Anti-Nef Light chain($V_L$)
$(G_4S)_3$ Linker
Anti-Nef Heavy chain($V_H$)
Cys-48
Cys-118
Cys-154
Cys-178
Cys-252
$^+H_3N$
C1
C2
C3
C4
C5
COO$^-$
$V_L$CDR1
$V_L$CDR2
$V_L$CDR3
$V_H$CDR1
$V_H$CDR2
$V_H$CDR3
Oxidation with GSH:GSSG
Anti-Nef Heavy chain ($V_H$)
Anti-Nef Light chain ($V_L$)
Refolded scFv
SH
Origin
Signal peptide
Carbenicillin resistance
pFB006
anti-Nef scFv
Linker
β-barrel
TEV cleavage site
Autodisplay
anti-Nef scFv
Outer membrane
TEV cleavage site
β-barrel
Lipoprotein

(b)

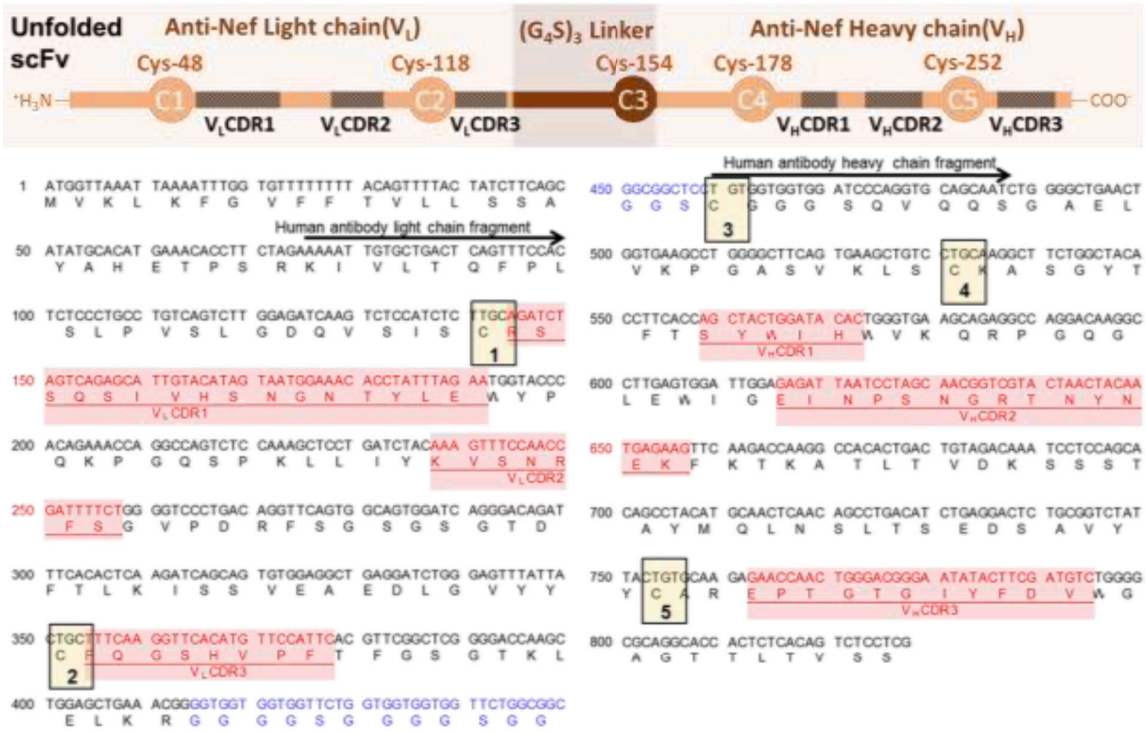
Unfolded scFv
Anti-Nef Light chain($V_L$)
$(G_4S)_3$ Linker
Anti-Nef Heavy chain($V_H$)
Cys-48
Cys-118
Cys-154
Cys-178
Cys-252
$^+H_3N$
COO$^-$
C1
C2
C3
C4
C5
$V_L$CDR1
$V_L$CDR2
$V_L$CDR3
$V_H$CDR1
$V_H$CDR2
$V_H$CDR3
Human antibody light chain fragment
Human antibody heavy chain fragment
1
2
3
4
5

Fig. 2

(a)

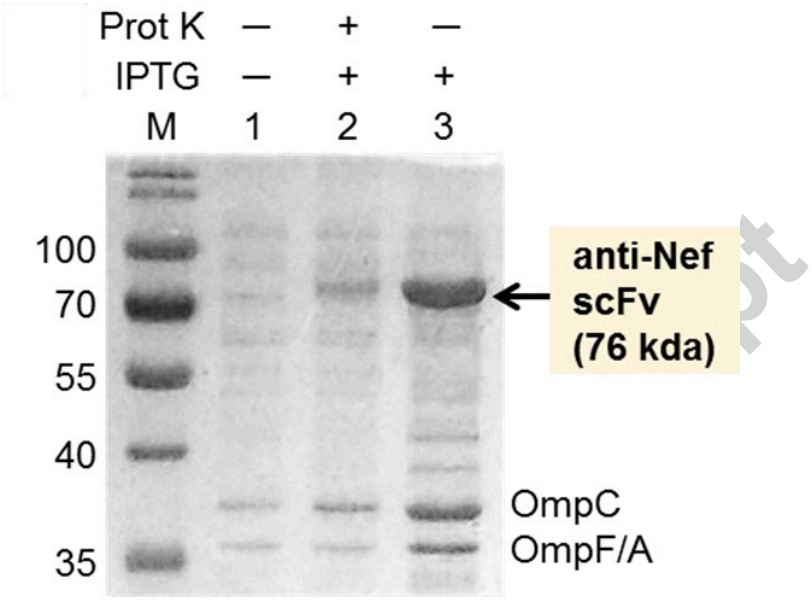
Prot K — + —
IPTG — + +
M 1 2 3
100
70
55
40
35
anti-Nef scFv (76 kda)
OmpC
OmpF/A

(b)

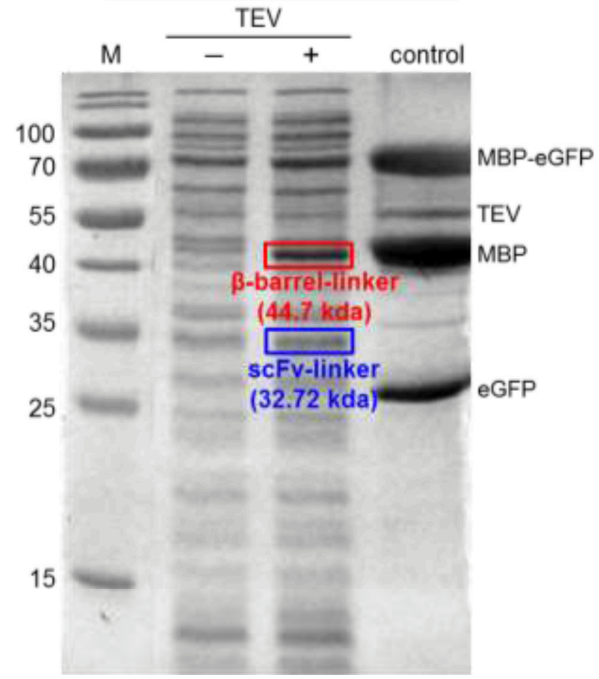
TEV
M — + control
100
70
55
40
35
25
15
MBP-eGFP
TEV
MBP
β-barrel-linker (44.7 kda)
scFv-linker (32.72 kda)
eGFP

Fig. 2(c)

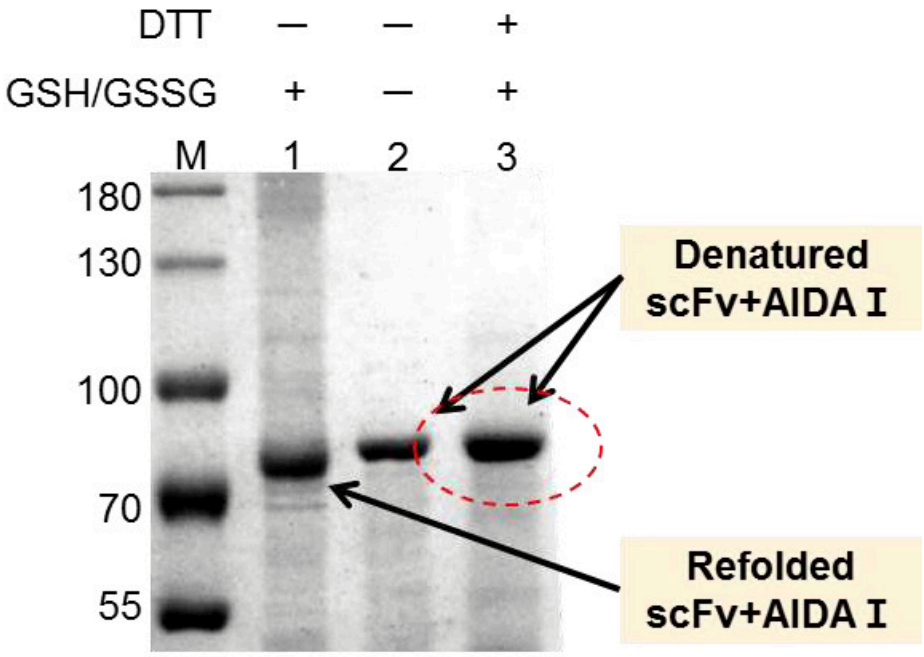

Fig. 3(a)

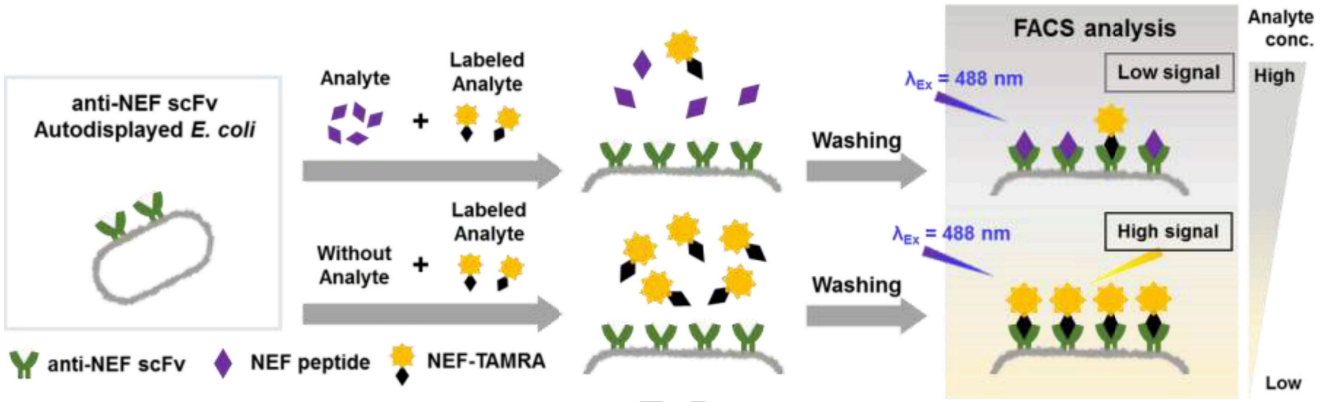

Fig. 3(b)

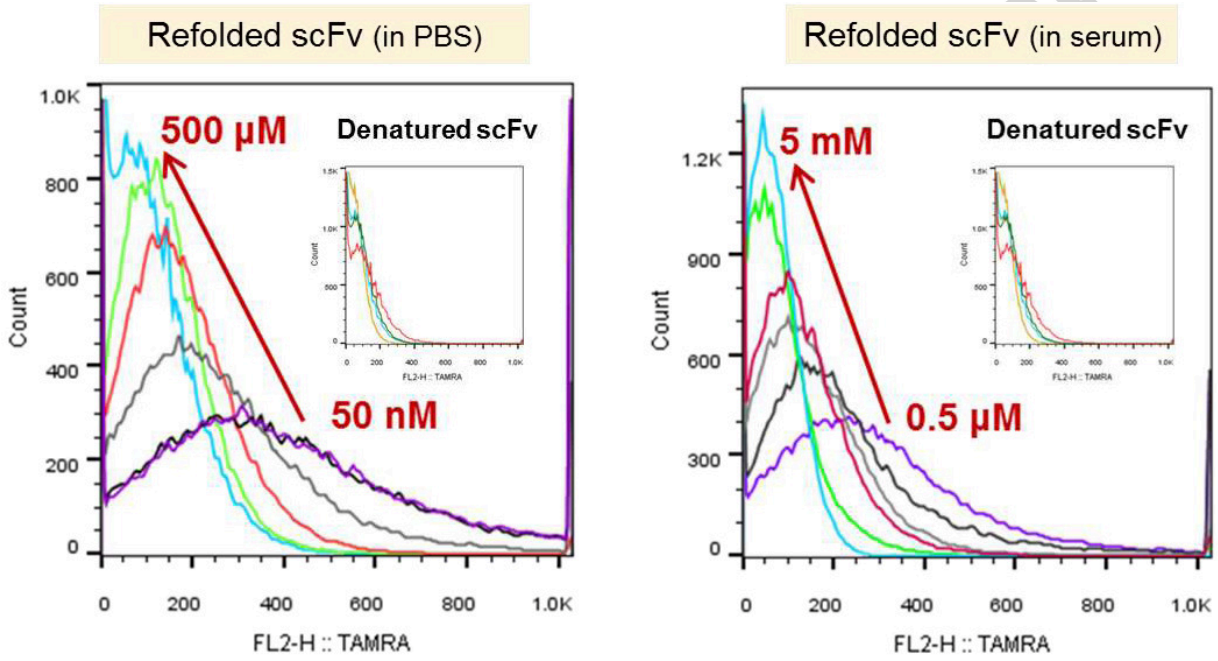

Fig. 3(c)

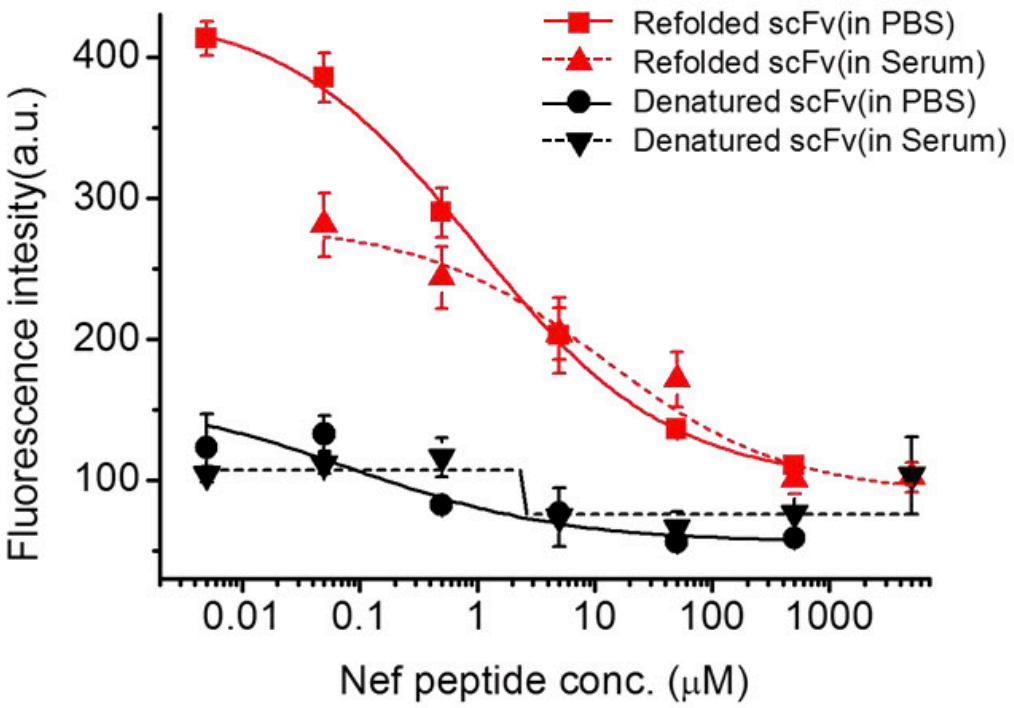

Fig. 3(d)

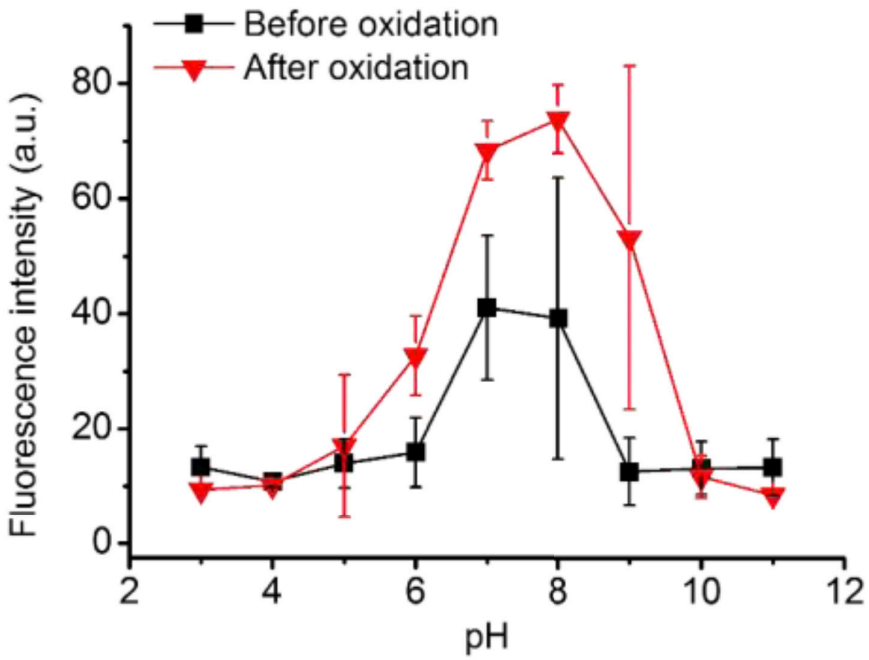

Fig. 4

(a)

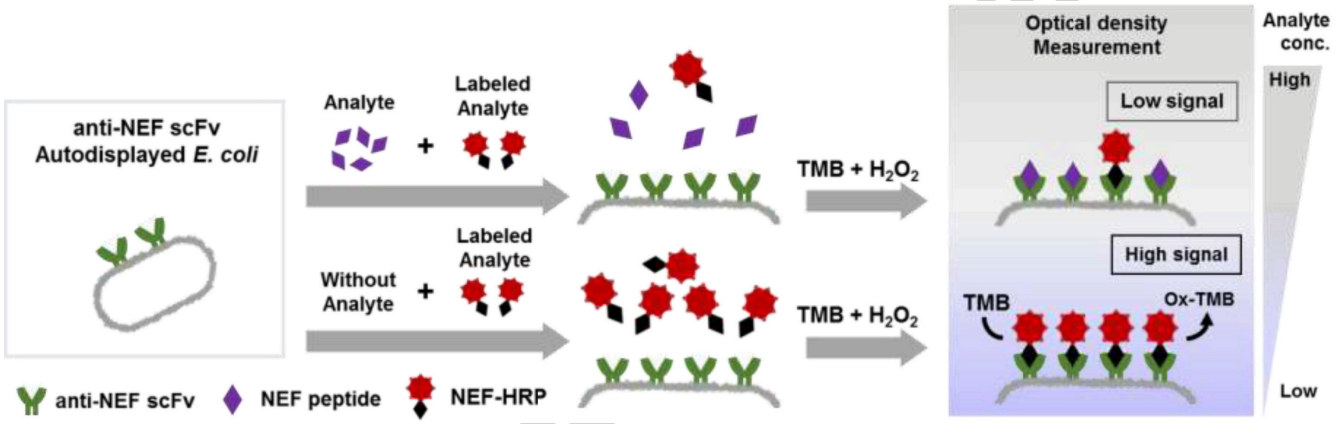

Fig. 4(b)

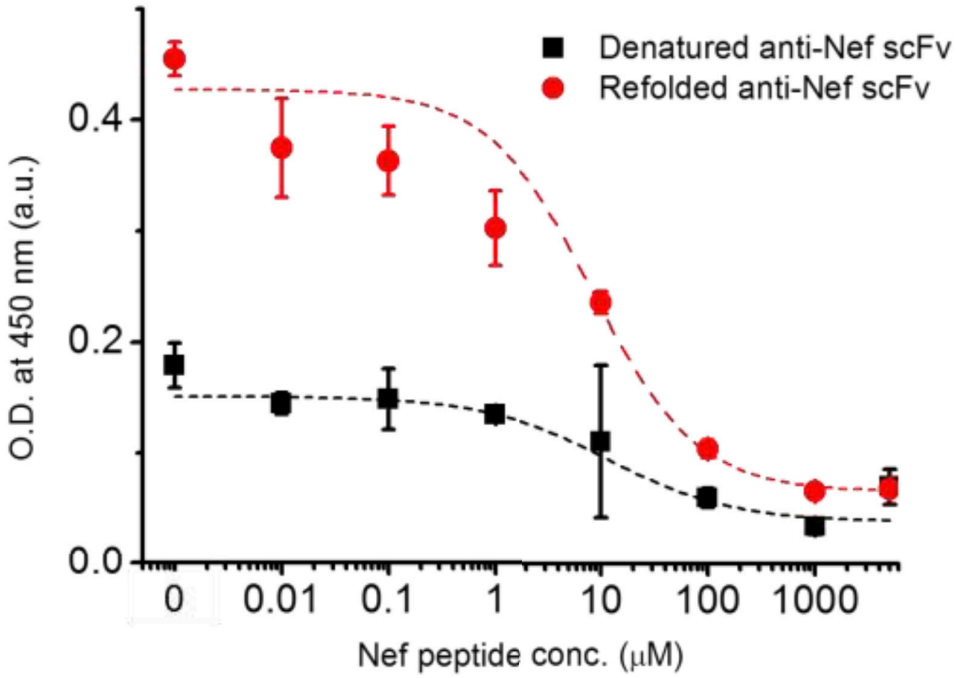

Fig. 5.

(a)

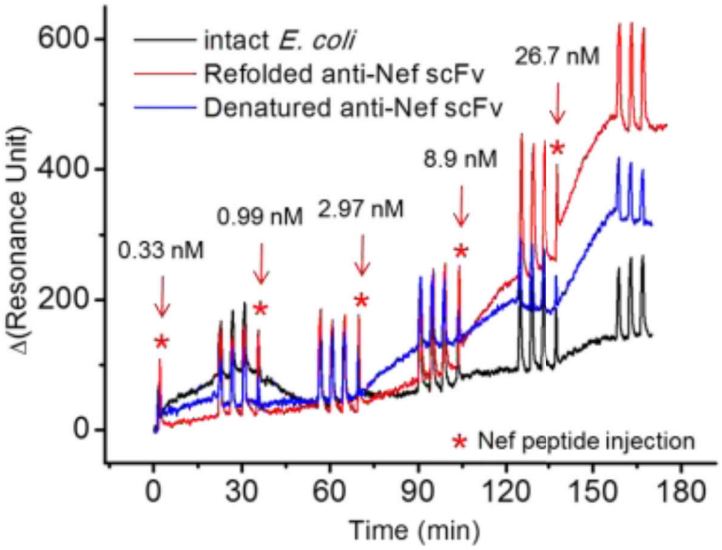
intact E. coli
Refolded anti-Nef scFv
Denatured anti-Nef scFv
0.33 nM
0.99 nM
2.97 nM
8.9 nM
26.7 nM
* Nef peptide injection
Δ(Resonance Unit)
Time (min)
0
200
400
600
0
30
60
90
120
150
180

(b)

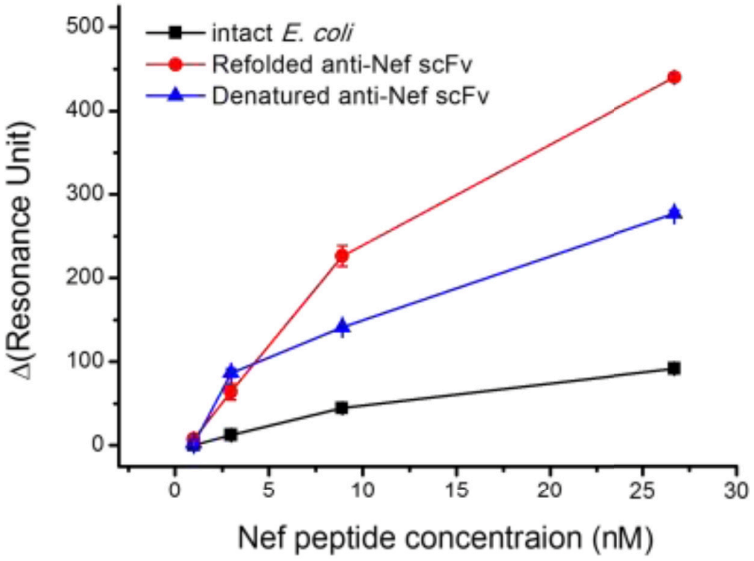
intact E. coli
Refolded anti-Nef scFv
Denatured anti-Nef scFv
Δ(Resonance Unit)
Nef peptide concentraion (nM)
0
100
200
300
400
500
0
5
10
15
20
25
30

Fig. 6(a)

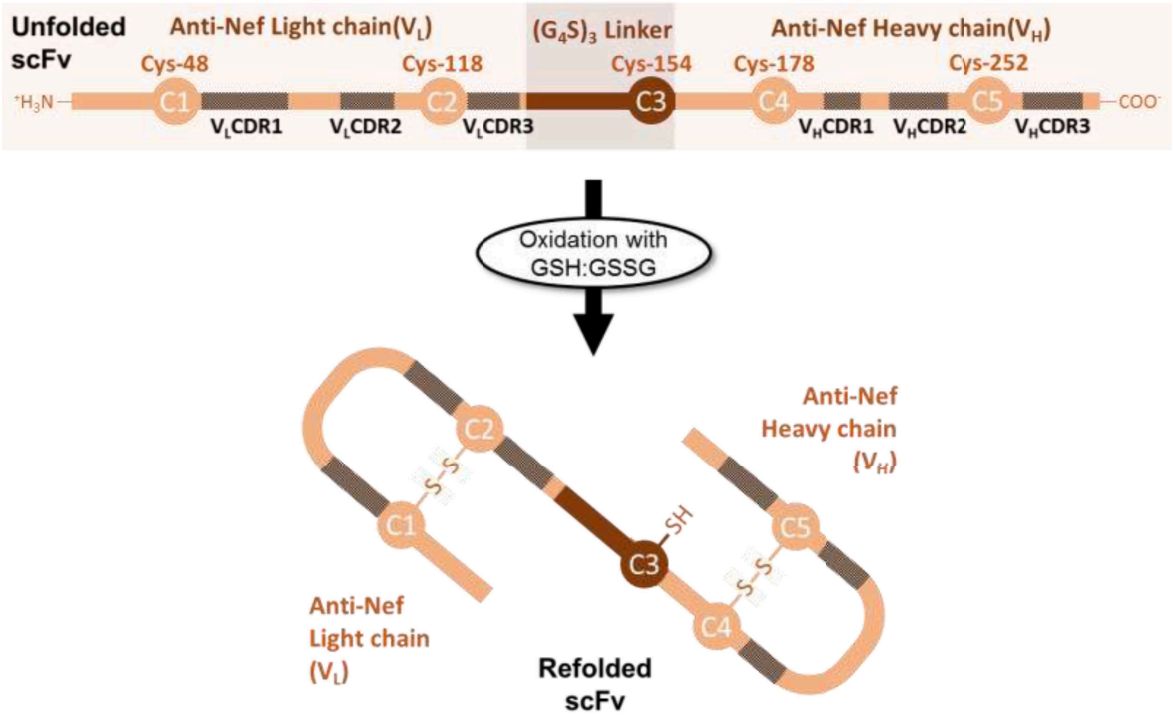
Unfolded scFv
Anti-Nef Light chain($V_L$)
$(G_4S)_3$ Linker
Anti-Nef Heavy chain($V_H$)
Cys-48
Cys-118
Cys-154
Cys-178
Cys-252
$^+H_3N$
C1
C2
C3
C4
C5
COO$^-$
$V_L$CDR1
$V_L$CDR2
$V_L$CDR3
$V_H$CDR1
$V_H$CDR2
$V_H$CDR3
Oxidation with GSH:GSSG
Anti-Nef Heavy chain ($V_H$)
Anti-Nef Light chain ($V_L$)
SH
Refolded scFv

Fig. 6(b)

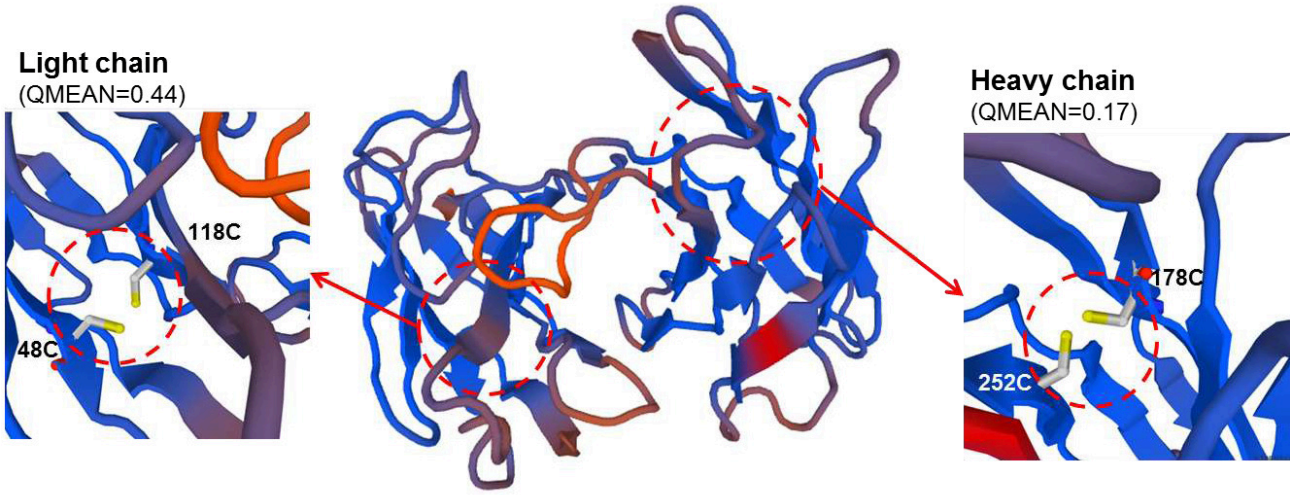

Fig. 6(c)

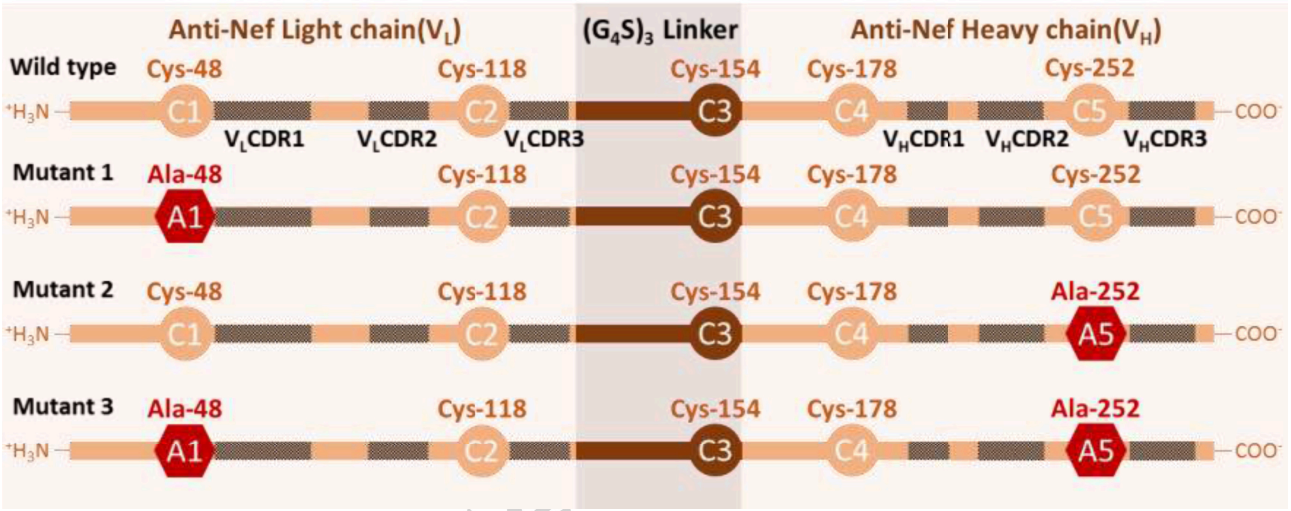

Fig. 6(d)

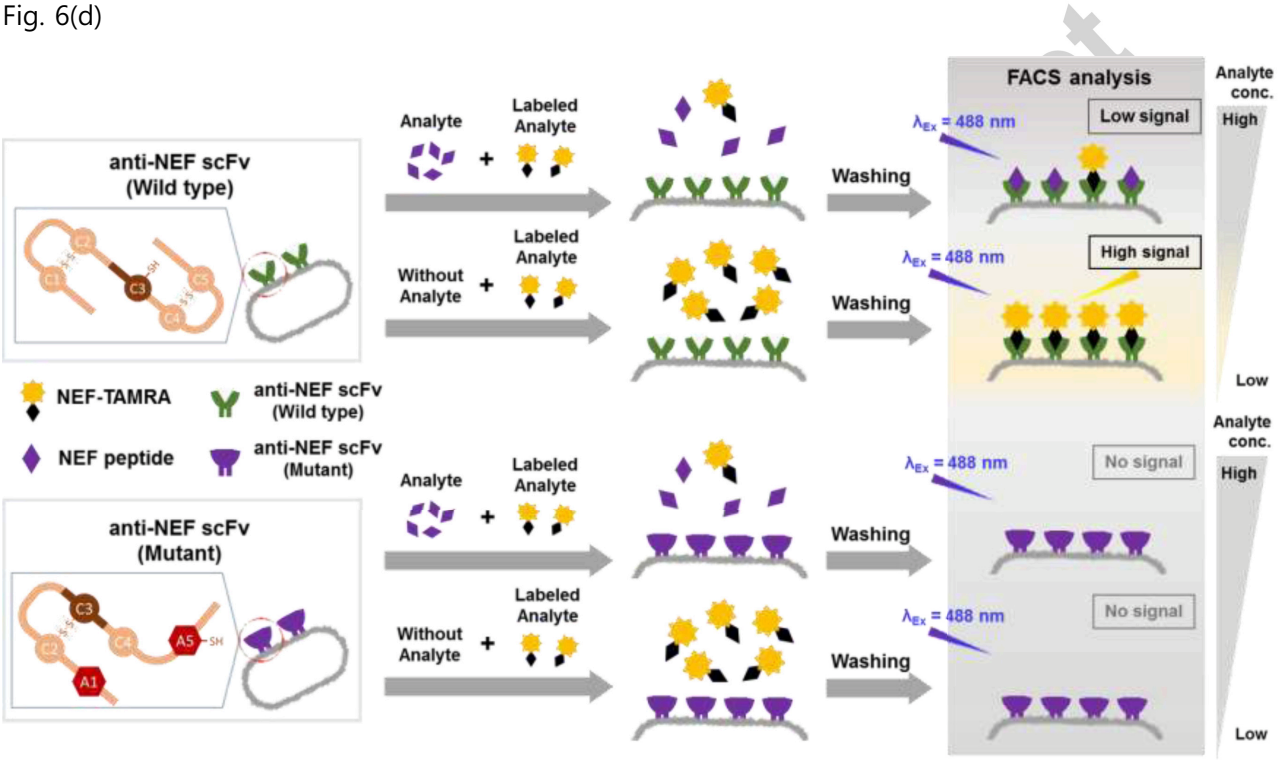

Fig. 6(e)